Physica Scripta

PAPER

Effect of DM Interaction in the charging process of a Heisenberg spin chain quantum battery

Sanah Rahman K* and **S Murugesh**

Department of Physics, Indian Institute of Space Science and Technology, Thiruvananthapuram - 695547, India

* Author to whom any correspondence should be addressed.

E-mail: sanahrahman.21@res.iist.ac.in **and** murugesh@iist.ac.in

RECEIVED
23 June 2024

REVISED
16 October 2024

ACCEPTED FOR PUBLICATION
21 November 2024

PUBLISHED
4 December 2024

Keywords: Heisenberg Spin Chain Quantum Battery, Dzyaloshinskii-Moriya Interaction, local and collective charging protocols, quantum energy fluctuations, anisotropic XYZ model

Abstract

We investigate the charging performance of an anisotropic XYZ model of Heisenberg Spin Chain Quantum Battery (HS QB) along with different components of Dzyaloshinskii-Moriya Interaction (DMI) for three cases - short range, long range and infinite range interactions. We find that the presence of DMI enhances the charging power and total stored energy of the QB considered here, when compared to HS QB in most of the cases, by considering both local and collective charging protocols. The maximum stored energy increases linearly with the number of spins (N). An extensive scaling of maximum charging power with the number of spins is obtained in which the maximum power approaches a scaling exponent $\alpha = 1.846$ for collective charging of the model consisting of Heisenberg spin chain with Y component of DMI under infinite range interactions. Finally, we optimize the performance of the battery by measuring the quantum energy fluctuations with in the system.

1. Introduction

Recent years have witnessed an outpouring of interest in the study and development of various new quantum technologies ranging from quantum thermal machines, quantum heat engines, quantum refrigerators, quantum supercapacitors, quantum batteries etc [1–5]. These technologies stem from the emerging field of quantum thermodynamics, which has the larger objective of giving a quantum mechanical description of the thermodynamic phenomena [6]. On the application side, one of the major objectives is to build quantum thermal machines, including quantum batteries, that exploit non-classical resources such as quantum coherence and entanglement. Studies on quantum batteries, especially, have gained much attention since the critical work by Alicki and Fannes [7]. *Quantum advantage*, often proves a substantial incentive in the pursuit of these technologies, just as it has been in other areas of earlier quantum technologies, be it quantum computation or communication. Quantum Batteries (QBs) are devices or systems that can store and supply energy which have a distinct quantum advantage when compared to their classical counterparts in atleast two aspects: a) faster charging rates, and b) possibly fully reversible charging [8]. Of these two, faster charging rates are possible critically due to entanglement among the quantum cells that make up the battery, a feature not possible in classical batteries [7]. In addition, it has been shown that if energy is stored in quantum many-body systems, entanglement generation also leads to faster work extraction [9].

The charging of a quantum battery can be accomplished using two broadly different protocols, global charging and parallel charging protocols [10]. In global charging protocol, the subsystems-*cells* of a battery are charged collectively by means of global entangling operations, which is also referred to as collective charging. Whereas in the case of parallel charging protocol, each subsystem of the battery is charged locally and independently of each other, similar to the charging of conventional batteries. Parallel charging of a quantum battery would yeild a charging power P that is linearly dependent on the number of cells in the quantum battery, N, collective charging on the other hand, which fundamentally invokes quantum entanglement among the cells,

can provide a maximum charging power $P \propto N^{\alpha}$, with the exponent $\alpha \geqslant 1$. Recently, Gyhm.et.al [11] have shown the upper bound on α to be 2. This theoretical result sets the limit for maximum charging power that can be attained by a quantum battery, and consequently sets in a search for the appropriate physical model governing the quantum battery that can yield us this maximum value for the exponent α. Over the last decade, several studies have focussed on the charging and discharging process in battery models [12, 13], and maximising work extraction(ergotropy) [14–16]. In recent years, many theoretical models of QBs have been proposed [17–33] and a few experimental realisations have also been reported since [34–39]. Numerous models based on spin systems have been reported in literature [40–45] of which Heisenberg Spin Chain (HS) based QB models especially garnered much attention for being among the simplest, yet versatile, conceivable quantum models [46–62].

In 1960, T. Moriya introduced an antisymmetric type of magnetic exchange interaction known as Dzyaloshinskii-Moriya Interaction (DMI) based on Anderson's superexchange formalism [63, 64]. This interaction accounts for the weak ferromagnetic behaviour of some antiferromagnets. The materials that lack inversion symmetry with strong spin–orbit coupling exhibit DMI, and hence this interaction originates from spin–orbit coupling. In magnetically ordered systems, this interaction leads to spin 'canting' and is of the form, $\sum_{i<j}^{n} \vec{\mathbf{D}}_{ij} \cdot (\vec{\mathbf{S}}_i \times \vec{\mathbf{S}}_j)$, where $\vec{\mathbf{S}}_i$ are the spin magnetic moments at each lattice site (subscript indexing the lattice site), $\vec{\mathbf{S}}_i = \frac{\hbar}{2}\vec{\sigma}_i$, where $\vec{\sigma}_i$ is Pauli spin operator corresponding to the lattice site i. $\vec{\mathbf{D}}_{ij}$ is a vector integral coefficient determined by the spatial part of the one-electron wavefunctions associated with the magnetic ions at sites i and j. In the case of Heisenberg spin chains with DM interactions, DMI competes with Heisenberg exchange interactions, leading to the formation of a noncollinear spin configuration in the ground state. This model was experimentally realized recently in two isostructural compounds of spin chain systems, $K_2CuSO_4Cl_2$ and $K_2CuSO_4Br_2$, which feature Heisenberg spin chains with uniform DMI [65].

In the present work, we investigate the charging performance of the anisotropic XYZ model of the Heisenberg Spin Chain Quantum Battery (HS QB), wherein the spins also interact through DMI with either short-range, long-range, or infinite-range interactions. The critical role of anisotropy in generating quantum correlations and entanglement is well realized by now. An isotropic Heisenberg spin chain does not generate either [58]. We consider two possible cases of charging: local (interacting) and global (collective) charging of spins, in order to compare the battery operation based on both charging protocols. In addition, we study the effect of different components of DMI (say, X, Y, and Z components) in the charging process of the quantum battery model.

We note that DMI has not been studied sufficiently in the context of QBs, although the inherently anisotropic interaction is known to influence quantum coherence and entanglement. By incorporating DMI into the Heisenberg spin chain model, we aim to investigate if this interaction can enhance the charging power and stored energy of QBs, and see how it compares to previously studied models. In a recent study, Zhang *et al* have investigated the performance of a two spin quantum battery with DMI, along with other spin-spin interactions [61]. Here, we have investigated the general N-spin quantum battery in the case of short-range, long-range and infinite range interactions, and particularly studied how the charging power scales with N.

This paper is organized as follows: In section 2, we introduce the battery model of the HS+DMI QB with relevant figures of merit to elucidate the battery performance. Then we consider the cases of short-range, long-range, and infinite-range interactions to plot the time evolution of total stored energy and the corresponding average power and then find the maximum stored energy and power as a function of the number of spins. We present a comparative study between HS+DMI QB and HS QB for different charging schemes by considering different components of DMI. The quantum advantage corresponding to both charging protocols, local (interacting) and collective charging, is calculated for infinite-range interactions. Then we measure the energy quantum fluctuations in section 3 under different interaction ranges for different charging cases by comparing the results with different QB models. Energy fluctuation is plotted versus time, and then the value of energy fluctuation at time that maximizes energy is calculated and plotted with the system size. Finally, we summarize the results in section 4.

2. Model of HS+DMI quantum battery

Our model QB consists of a one-dimensional anisotropic XYZ Heisenberg spin chain, along with an added DM interaction term. A constant external magnetic field acting along the z-direction plays the role of a polarization field, with interaction energy H_z, given by

$$H_z = \frac{\omega_z}{2}\sum_{i=1}^{N} \sigma_i^z, \tag{1}$$

where ω_z represents the strength of magnetic field (with units of energy) after an appropriate scaling. We shall consider two types of charging protocols in a closed quantum system, namely, local and collective charging schemes. In our model, we employ local charging for an interacting spin system, i.e., the system consists of an "N" spin chain with both Heisenberg and DM interactions prior to the charging operations. More specifically, we consider a QB based on quantum-interacting spin model which is charged via a local external uniform magnetic field. The local charging of spin chain is achieved using a direct charging protocol [8, 58, 59, 66] in which the hamiltonian H_z is turned off and the hamiltonian due to the local external magnetic field along the y direction, H_y, given by

$$H_y = \frac{\omega_y}{2}\sum_{i=1}^{N}\sigma_i^y \tag{2}$$

is applied during the charging process, where ω_y is the strength of the applied field. The total hamiltonian of the system for local charging can be written as

$$H_L(t) = H_L^{(0)} + \lambda(t)(H_L^{(1)} - H_z) \tag{3}$$

where,

$$H_L^{(0)} = H_z + H_{HS} + H_{DMI} \tag{4}$$

$$H_L^{(1)} = H_y \tag{5}$$

$H_L^{(0)}$ is the base or system hamiltonian and $H_L^{(1)}$ is the charging hamiltonian. H_{HS} and H_{DMI} are the hamiltonians corresponding to the Heisenberg and DM interactions given by

$$H_{HS} = \frac{1}{4}\sum_{i<j}^{N} g_{ij}[(1+\gamma)\sigma_i^x\sigma_j^x + (1-\gamma)\sigma_i^y\sigma_j^y + \Delta\sigma_i^z\sigma_j^z] \tag{6}$$

$$H_{DMI} = \sum_{i<j}^{N}\overrightarrow{\mathbf{D}}_{ij}\cdot(\overrightarrow{\sigma_i}\times\overrightarrow{\sigma_j}) \tag{7}$$

where σ_i^x, σ_i^y, σ_i^z are the Pauli spin operators at the corresponding site, indexed by the subscript i. γ and Δ are the anisotropy parameters. Here, $\lambda(t)$ is a step function: $\lambda(t) = 1$ for $t \in [0, T]$ and zero otherwise, which acts as a switch for the charging process, with T denoting the charging time. Due to the presence of intrinsic interactions between the spins before the charging process, the initial state of the battery can become entangled. But local charging negates the possibility of entanglement generation during the charging process. Whereas in the case of collective charging, the system consists of N independent spins which are collectively charged via global operations that creates the possibility of generation of entanglement between the spins during the charging process. In our model, the battery is charged by introducing a sudden nonequilibrium quantum quench $H_C^{(1)}$ which constitutes the Heisenberg spin-spin interactions and DM interaction for the collective charging protocol [10, 56, 57, 67]. The corresponding form of the total hamiltonian of the system is given by

$$H_C(t) = H_C^{(0)} + \lambda(t)H_C^{(1)} \tag{8}$$

where,

$$H_C^{(0)} = H_z \tag{9}$$

$$H_C^{(1)} = H_{HS} + H_{DMI} \tag{10}$$

Here $H_C^{(0)}$ is the static hamiltonian and $H_C^{(1)}$ is the interaction hamiltonian. Comparing with the local charging protocol, it may be noted that the energy stored in the battery after charging will be the expectation value of the paramagnetic hamiltonian, $H_C^{(0)}$ in equation (8) in the case of collective charging, whereas with local charging it would be the expectation value of the hamiltonian $H_L^{(0)}$ in equation (3), which includes the spin-spin interactions. In the following, we shall consider three independent cases for the strength of interactions: short-range (SR), long-range (LR) and infinite-range (IR) interactions given by

$$D_{ij}^{SR} = D\delta_{i,j-1},\quad D_{ij}^{LR} = \frac{D}{|i-j|^q},\quad D_{ij}^{IR} = D(\text{or } q=0), \tag{11}$$

$$g_{ij}^{SR} = g\delta_{i,j-1},\quad g_{ij}^{LR} = \frac{g}{|i-j|^m},\quad g_{ij}^{IR} = g(\ m=0), \tag{12}$$

where D, g are real constants and $q, m \geqslant 0$. g is the spin-spin interaction strength and D is the DM interaction strength. Here in our model, the direction of polarization field, H_z is taken along negative z direction and hence each spin is prepared in the ground state, $|G\rangle = |\downarrow\rangle$. Therefore, we consider the initial state of the battery as the ferromagnetic ground state as follows.

$$|\Psi(0)\rangle = |G, G, ...,G\rangle = |\downarrow\downarrow.....\downarrow\rangle \tag{13}$$

Then the wave function of the system evolves with time t which is given by

$$|\Psi(t)\rangle = e^{-iHt/\hbar}|\Psi(0)\rangle \tag{14}$$

Here H represents the time independent total hamiltonian of the system, corresponding to a given charging protocol (ie, either local charging (H_L) or collective charging (H_C)). It must be noted that the total hamiltonian is time independent during the entire charging phase. For convenience, we shall set $\hbar = 1$ all along. The total stored energy by the battery at a particular instant t is given by

$$E(t) = \langle\Psi(t)|\ H^{(0)}|\Psi(t)\rangle - \langle\Psi(0)|\ H^{(0)}|\Psi(0)\rangle \tag{15}$$

where $H^{(0)}$ is the system hamiltonian corresponding to a given charging protocol. The corresponding average power for a given time t is given by

$$P(t) = \frac{E(t)}{t} \tag{16}$$

The maximum stored energy from the battery (at time t_E) is

$$E_{max} \equiv \max_t(E(t)) = E(t_E) \tag{17}$$

Similarly the maximum power (at time t_P) is

$$P_{max} \equiv \max_t(P(t)) = P(t_P) \tag{18}$$

In this paper, the calculations are done and coded in PYTHON using QuTiP library [68].

2.1. Short range interactions

Consider the nearest neighbour (NN) interactions between the spins of the battery. The corresponding hamiltonians for local and collective charging are given by equations (3) and (8) where

$$H_{HS} = \frac{g}{4}\sum_{i=1}^{N-1}[(1+\gamma)\sigma_i^x\sigma_{i+1}^x + (1-\gamma)\sigma_i^y\sigma_{i+1}^y + \Delta\sigma_i^z\sigma_{i+1}^z] \tag{19}$$

For simplicity, we restrict the direction of DMI along one direction (say, X, Y or Z direction). Here we study and compare the effects of three different components of DMI (ie, in the X, Y and Z direction) in the charging process of the battery. The corresponding hamiltonians are given by

$$H_{DMI-x} = D_x\sum_{i=1}^{N-1}(\sigma_i^y\sigma_{i+1}^z - \sigma_i^z\sigma_{i+1}^y) \tag{20}$$

$$H_{DMI-y} = D_y\sum_{i=1}^{N-1}(\sigma_i^z\sigma_{i+1}^x - \sigma_i^x\sigma_{i+1}^z) \tag{21}$$

$$H_{DMI-z} = D_z\sum_{i=1}^{N-1}(\sigma_i^x\sigma_{i+1}^y - \sigma_i^y\sigma_{i+1}^x) \tag{22}$$

In order to analyse the effect of different components of DMI in the charging process of QB, the time evolution of total stored energy by the QB and the corresponding average power are plotted as shown in figures 1 and 2 for different charging cases and for different components of DMI. Here we also give the results of HS QB for comparison. In this paper, all plots have same parameters $N = 10, g = \pm 1, D_x = 1, D_y = 1, D_z = 1, \omega_z = 1, \omega_y = 1, \gamma = 0.5, \Delta = 2$ unless mentioned otherwise. We have plotted energy and power for both ferromagnetic case ($g = -1$) and anti-ferromagnetic case ($g = 1$) starting from the same initial state. From the figure 1, it is clear that for HS QB with X and Y components of DMI (ie, HS+DMI-x QB and HS+DMI-y QB), the total stored energy by the QB enhances as compared to HS QB in the case of collective charging by considering Nearest-Neighbour (NN) interactions and the corresponding increase in energy is more prominent in the ferromagnetic case. But for local charging, there is only notable increase in energy in the case of HS+DMI-x QB (anti-ferromagnetic case). Whereas in the case of HS QB with Z component of DMI (ie, HS+DMI-z QB), no significant change is observed in the case of energy compared to HS QB for both charging protocols. Figure 2 plots the time evolution of the average charging power of the QB. It clearly demonstrates that there is increment in power for both HS +DMI-x QB and HS+DMI-y QB compared to HS QB for all the cases considered. Whereas in the case of HS +DMI-z QB, there is no change observed in the case of power compared to HS QB in which the trend is similar with that of energy.

We then find the maximum stored energy ($E_{\max}$) and the maximum charging power ($P_{\max}$) as a function of total number of spins (N) for different charging cases and for different components of DMI and the results are plotted for anti-ferromagnetic case ($g = 1$) as shown in figures 3 and 4. Here we have taken $N = 1, 2. . . . . 20$ spins for demonstrating the results.

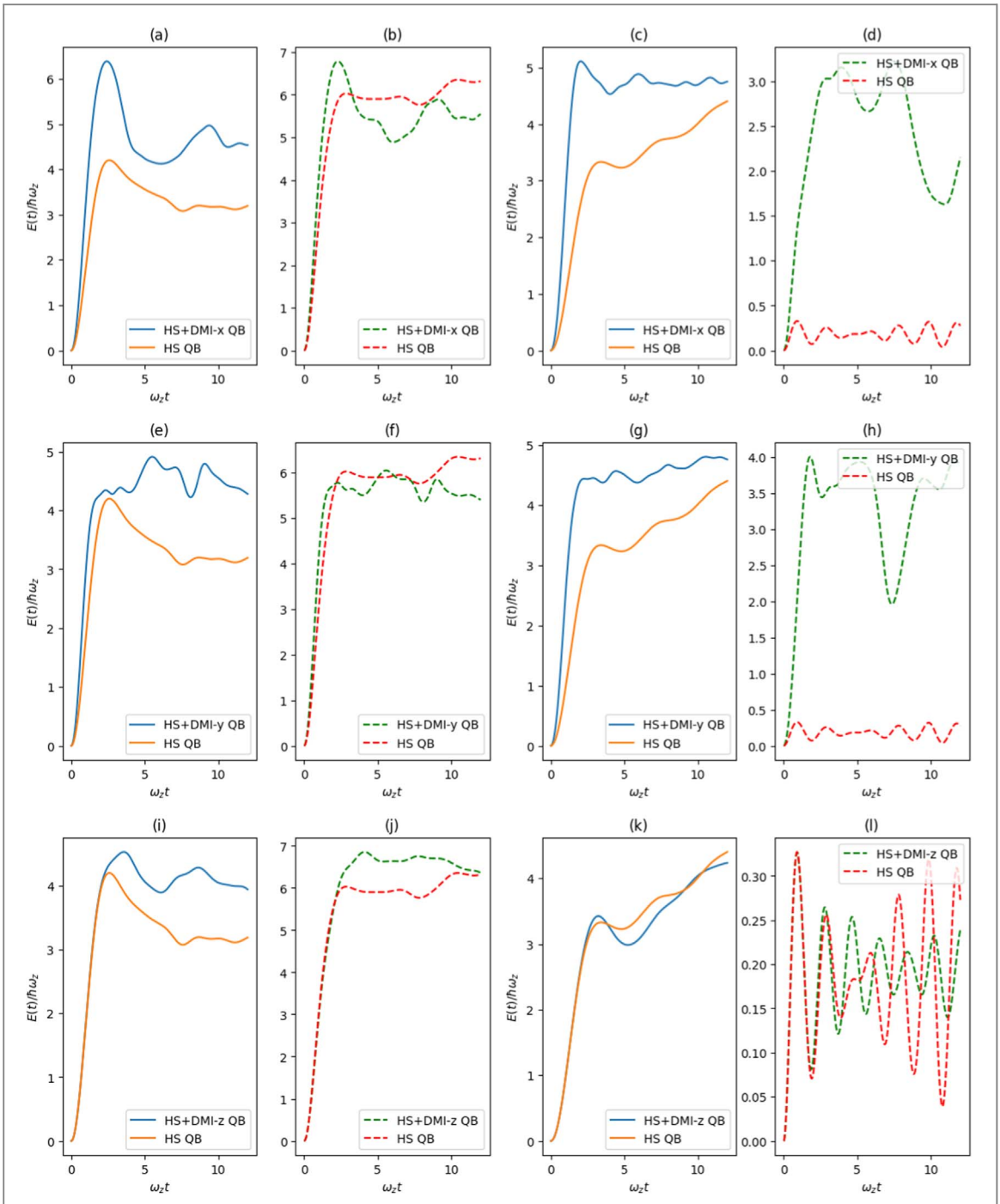

Figure 1. Total stored energy as a function of time for X, Y and Z components of DMI under short range interactions. (a), (b), (e), (f), (i) and (j) for local charging case and (c), (d), (g), (h), (k) and (l) for collective charging case. The blue-orange solid line plot for $g = 1$ and green-red dotted line plot for $g = -1$, respectively. In this paper, all plots have same parameters $N = 10, g = \pm 1, D_x = 1, D_y = 1, D_z = 1, \omega_z = 1, \omega_y = 1, \gamma = 0.5, \Delta = 2$ unless mentioned otherwise.

It shows that the maximum stored energy and maximum charging power have correlation with N and get enhanced with the number of spins. But compared to HS QB, notable difference is observed only in the case of HS+DMI-x QB and HS+DMI-y QB for both charging protocols like the previous result. Whereas in the case of HS+DMI-z QB, DMI-z component does not impart any significant effect on the performance of the battery.

The maximum stored energy scales linearly with the number of spins. Hence in the case of short range interactions, no significant quantum speed up is observed, but the presence of DMI-x and DMI-y components enhances the charging power and energy stored by the QB.

2.2. Long range interactions

In an earlier work on spin-chain QB [58], it is shown that the presence of interactions between spins leads to the potential quantum advantage and this advantage is super extensive for long range interactions. Motivated by this

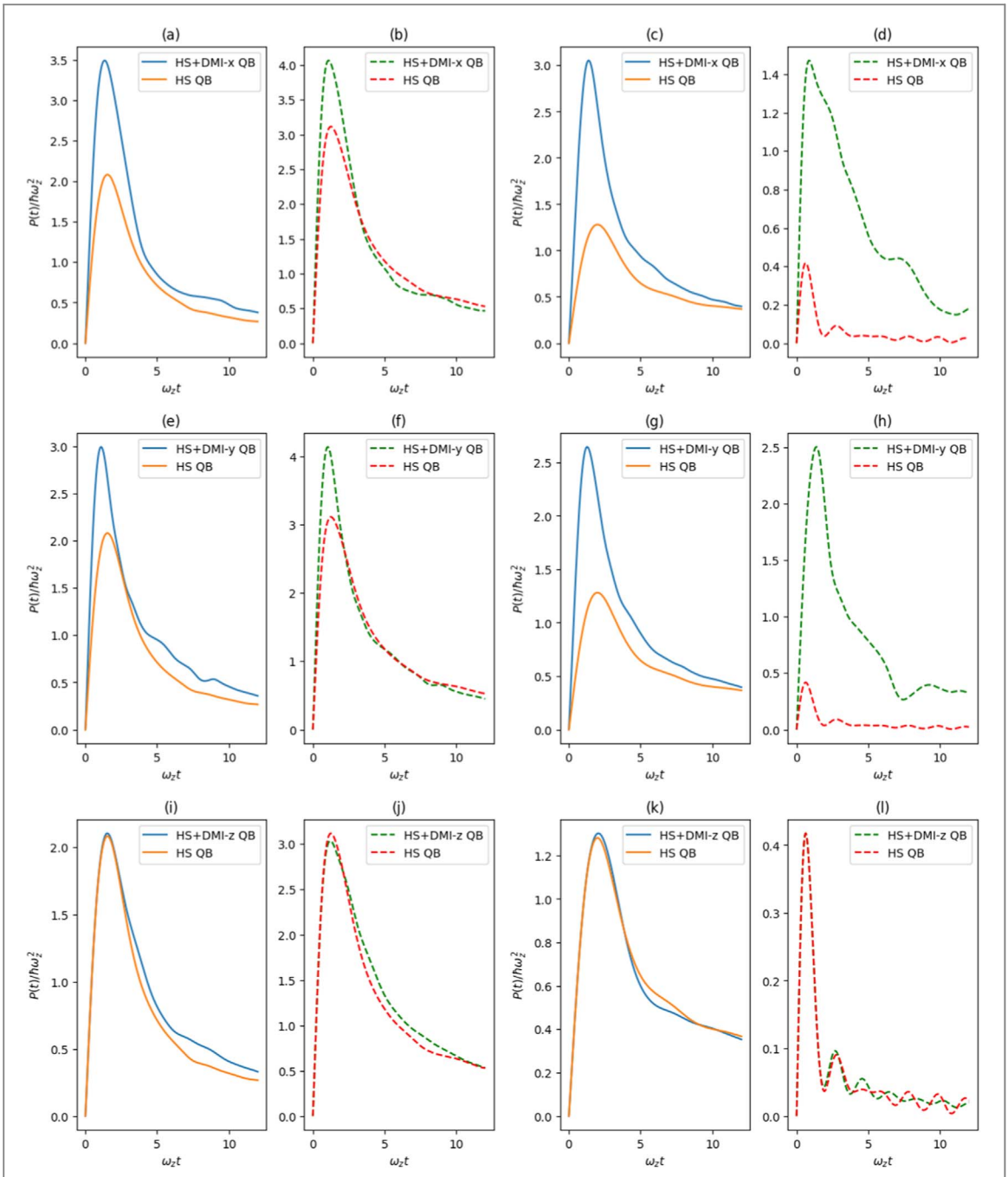

Figure 2. Average power as a function of time for X, Y and Z components of DMI under short range interactions. (a), (b), (e), (f), (i) and (j) for local charging case and (c), (d), (g), (h), (k) and (l) for collective charging case.

idea, we now analyse the effect of different components of DMI in the performance of a HS QB under long range interactions, where each spin interact with every other spins but the interaction decays with distance as a power law, given by equations (11) and (12). The hamiltonians corresponding to long range interactions are given by equations (3) and (8), where

$$H_{HS} = \frac{1}{4}\sum_{i<j}^{N} \frac{g}{|i-j|}[(1+\gamma)\sigma_i^x\sigma_j^x + (1-\gamma)\sigma_i^y\sigma_j^y + \Delta\sigma_i^z\sigma_j^z] \tag{23}$$

The hamiltonians corresponding to DMI for X, Y and Z components are

$$H_{DMI-x} = \sum_{i<j}^{N} \frac{D_x}{|i-j|}(\sigma_i^y\sigma_j^z - \sigma_i^z\sigma_j^y) \tag{24}$$

$$H_{DMI-y} = \sum_{i<j}^{N} \frac{D_y}{|i-j|}(\sigma_i^z\sigma_j^x - \sigma_i^x\sigma_j^z) \tag{25}$$

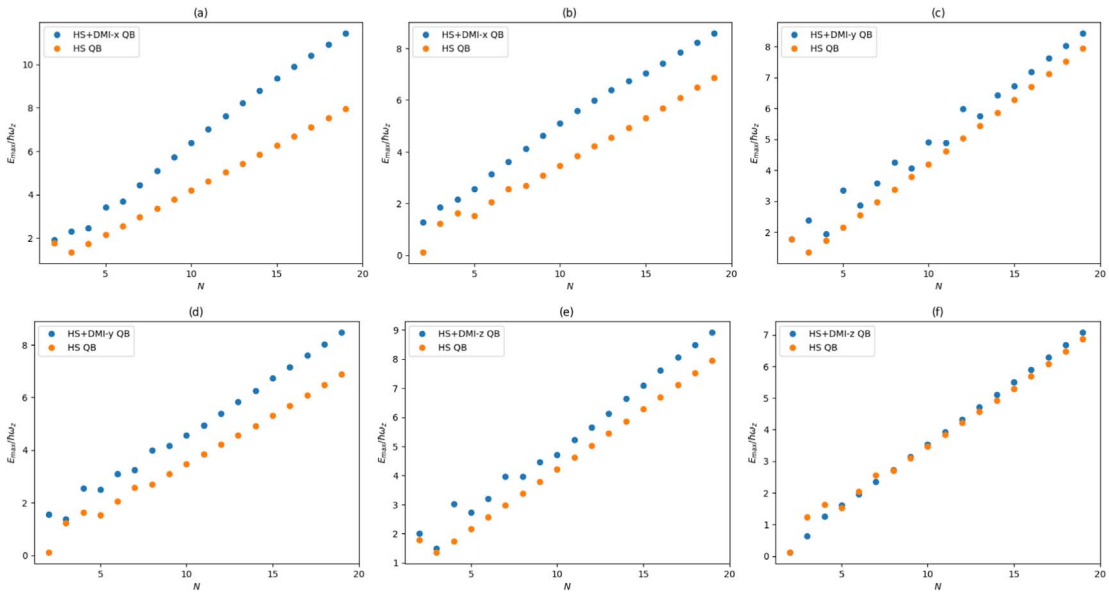

Figure 3. Maximum stored energy vs N for X, Y and Z components of DMI under short range interactions. (a), (c) and (e) for local charging case and (b), (d) and (f) for collective charging case. The HS+DMI QB (blue dot line) and HS QB (orange dot line), respectively.

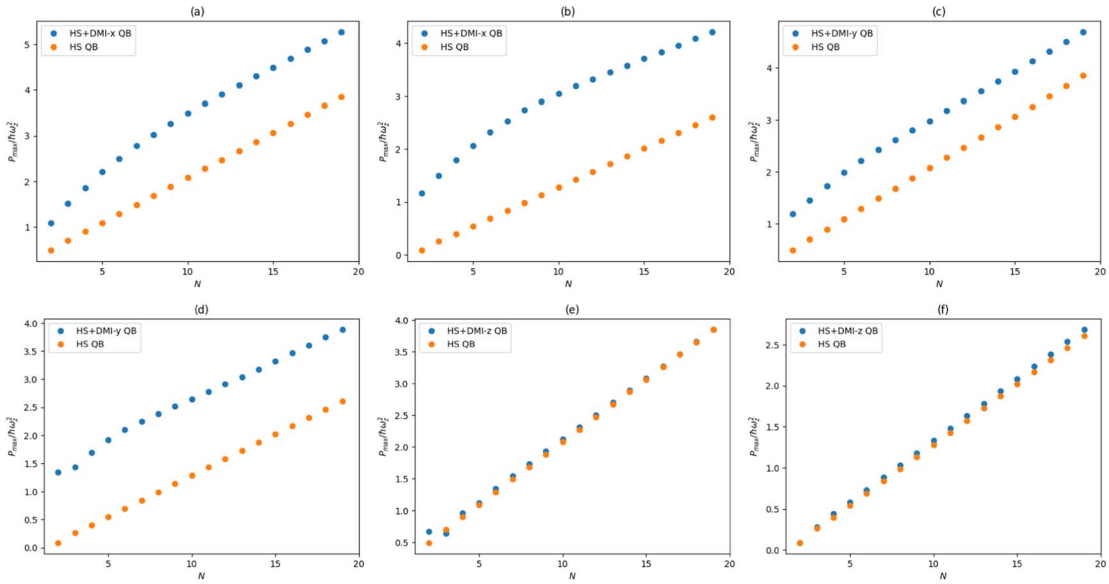

Figure 4. Maximum power vs N for X, Y and Z components of DMI under short range interactions. (a), (c) and (e) for local charging case and (b), (d) and (f) for collective charging case.

$$H_{DMI-z} = \sum_{i<j}^{N} \frac{D_z}{|i-j|}(\sigma_i^x \sigma_j^y - \sigma_i^y \sigma_j^x) \tag{26}$$

The time evolution of total stored energy by the QB and the corresponding average power are plotted as shown in figures 5 and 6 for different charging cases and for different components of DMI.

From the figure, we can conclude that for HS+DMI-x QB and HS+DMI-y QB, the total stored energy and power is significantly enhanced for both the charging cases compared to HS QB. Whereas in the case of HS +DMI-z QB, energy is enhanced for both charging schemes, but there is a decline in power in almost all cases except for the anti-ferromagnetic case of local charging as compared to HS QB.

The maximum stored energy ($E_{\max}$) and the maximum charging power ($P_{\max}$) of the battery are calculated as a function of total number of spins (N) for different charging cases and for different components of DMI and the results are shown in figures 7 and 8. The maximum stored energy and maximum charging power have clear correlation with the number of spins in the case of HS+DMI-x QB and HS+DMI-y QB for both charging

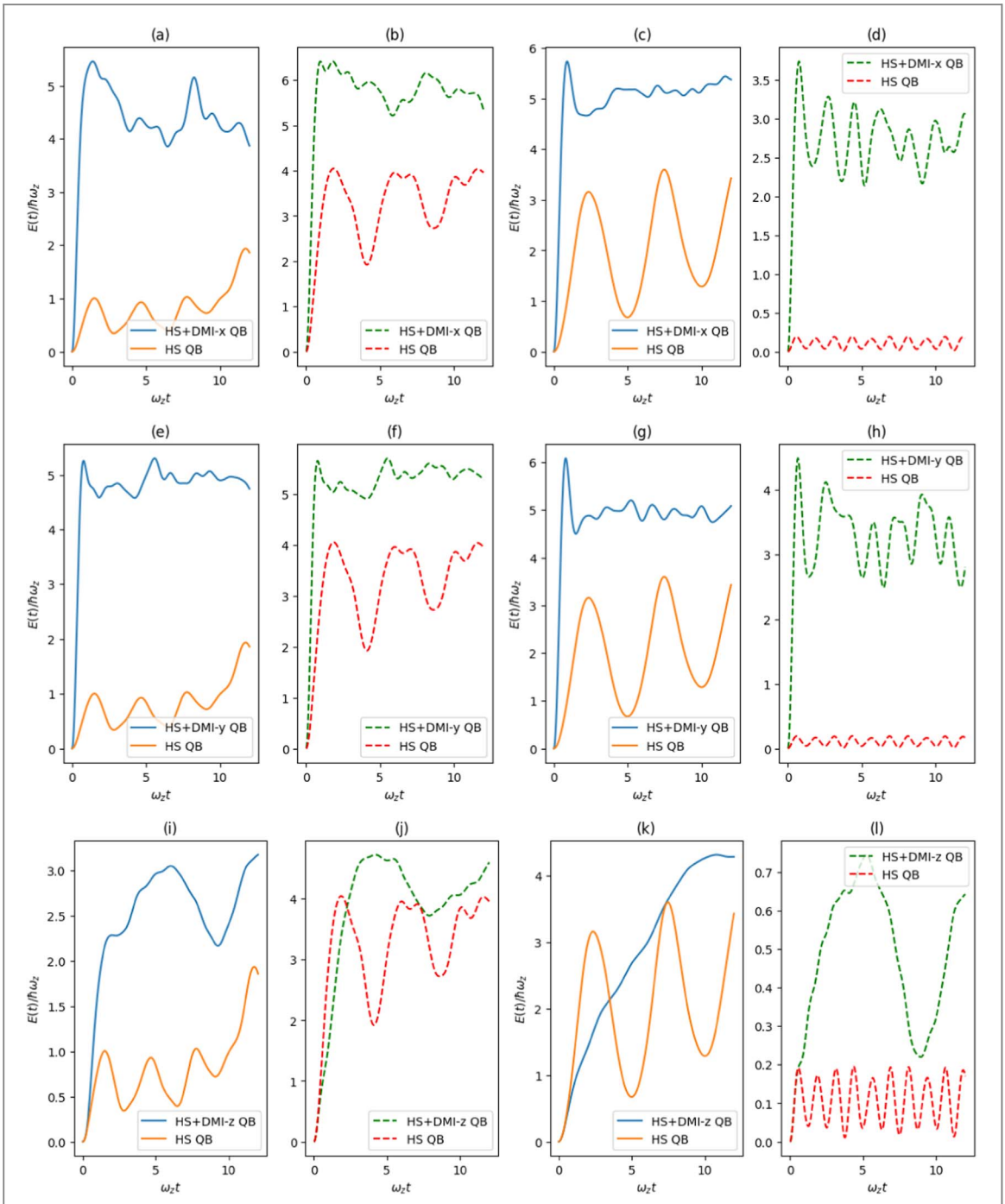

Figure 5. Total stored energy as a function of time for X, Y and Z components of DMI under long range interactions. (a), (b), (e), (f), (i) and (j) for local charging case and (c), (d), (g), (h), (k) and (l) for collective charging case.

protocols. Whereas in the case of HS+DMI-z QB, both $E_{\max}$ and $P_{\max}$ enhances with the number of spins compared to HS QB in the case of local charging, but in the case of collective charging, $E_{\max}$ and $P_{\max}$ enhances with N but at a slower rate compared to HS QB.

In addition, $E_{\max}$ increases almost linearly and shows some regularity with the number of spins. In the case of long range interactions, both energy and power are significantly enhanced for HS+DMI-x QB, whereas for HS+DMI-z QB, a significant enhancement in energy and power is only witnessed in the case of local charging.

2.3. Infinite range interactions

Towards the quest for obtaining the largest enhancement in power, we now consider infinite range interactions between the spins of the battery, where each spin interact with every other spins with same magnitude. The hamiltonians corresponding to infinite range interactions are given by equations (3) and (8), where

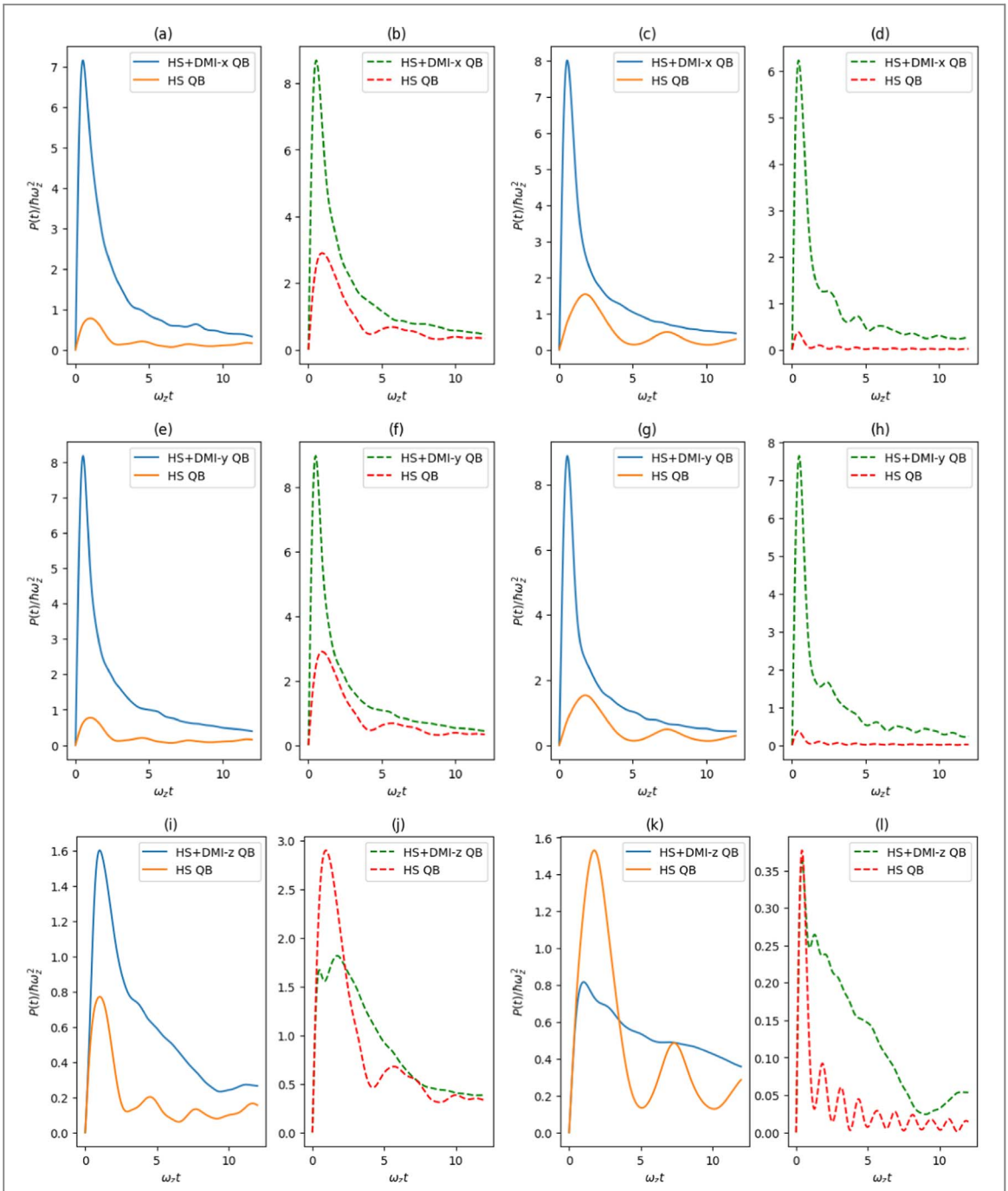

Figure 6. Average power as a function of time for X, Y and Z components of DMI under long range interactions. (a), (b), (e), (f), (i) and (j) for local charging case and (c), (d), (g), (h), (k) and (l) for collective charging case.

$$H_{HS} = \frac{g}{4}\sum_{i<j}^{N}[(1+\gamma)\sigma_i^x\sigma_j^x + (1-\gamma)\sigma_i^y\sigma_j^y + \Delta\sigma_i^z\sigma_j^z] \tag{27}$$

The hamiltonians corresponding to DMI for X, Y and Z components are

$$H_{DMI-x} = D_x\sum_{i<j}^{N}(\sigma_i^y\sigma_j^z - \sigma_i^z\sigma_j^y) \tag{28}$$

$$H_{DMI-y} = D_x\sum_{i<j}^{N}(\sigma_i^z\sigma_j^x - \sigma_i^x\sigma_j^z) \tag{29}$$

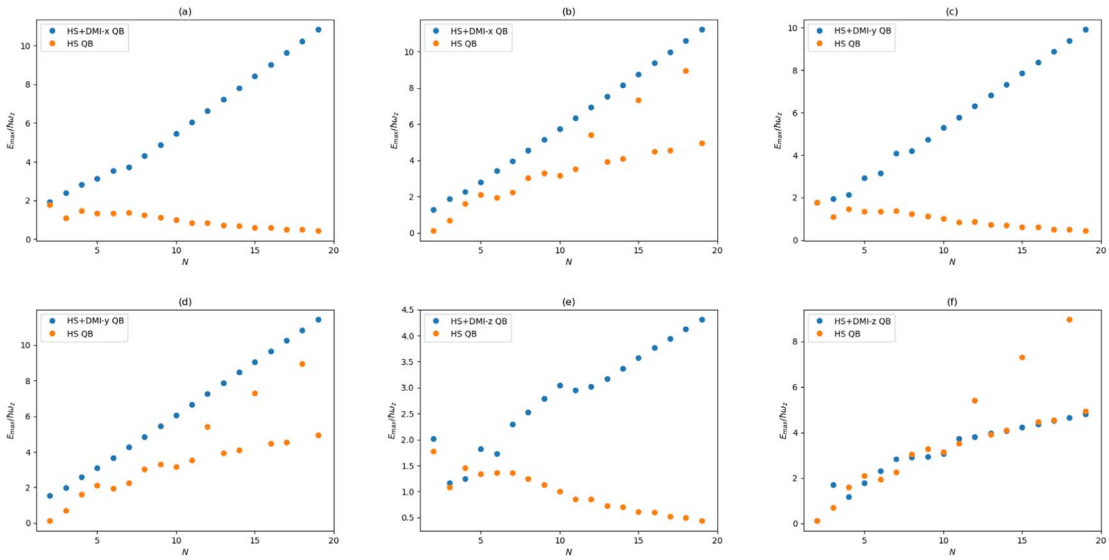

Figure 7. Maximum stored energy vs N for X, Y and Z components of DMI under long range interactions. (a), (c) and (e) for local charging case and (b), (d) and (f) for collective charging case.

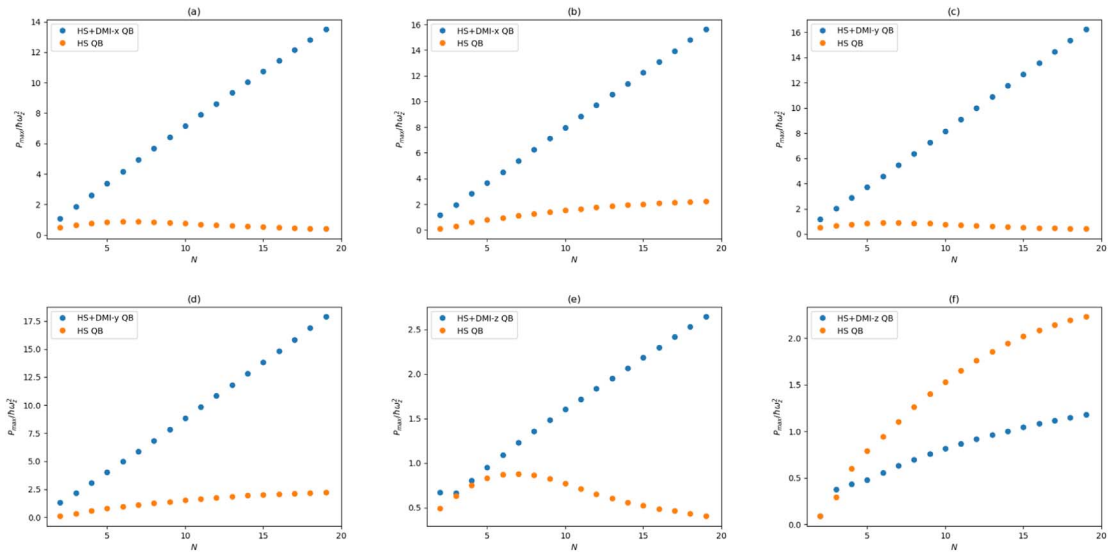

Figure 8. Maximum power vs N for X, Y and Z components of DMI under long range interactions. (a), (c) and (e) for local charging case and (b), (d) and (f) for collective charging case.

$$H_{DMI-z} = D_z \sum_{i<j}^{N} (\sigma_i^x \sigma_j^y - \sigma_i^y \sigma_j^x) \tag{30}$$

Using collective spin operator, $J_\theta = \frac{\hbar}{2}\sum_i^N \sigma_i^\theta$, where $\theta = x, y, z$, (1) and (2) become

$$H_z = hJ_z \tag{31}$$

$$H_y = \omega J_y \tag{32}$$

Then (27) can be rewritten in terms of collective spin operators as

$$H_{HS} = g\,[J_x^2 + J_y^2 + \gamma(J_x^2 - J_y^2) + \Delta J_z^2] \tag{33}$$

Using ladder operators, $J_\pm = J_x \pm iJ_y$, (33) becomes

$$H_{HS} = \frac{g}{2}[J_+J_- + J_-J_+ + \gamma(J_+^2 + J_-^2) + \Delta J_z^2] \tag{34}$$

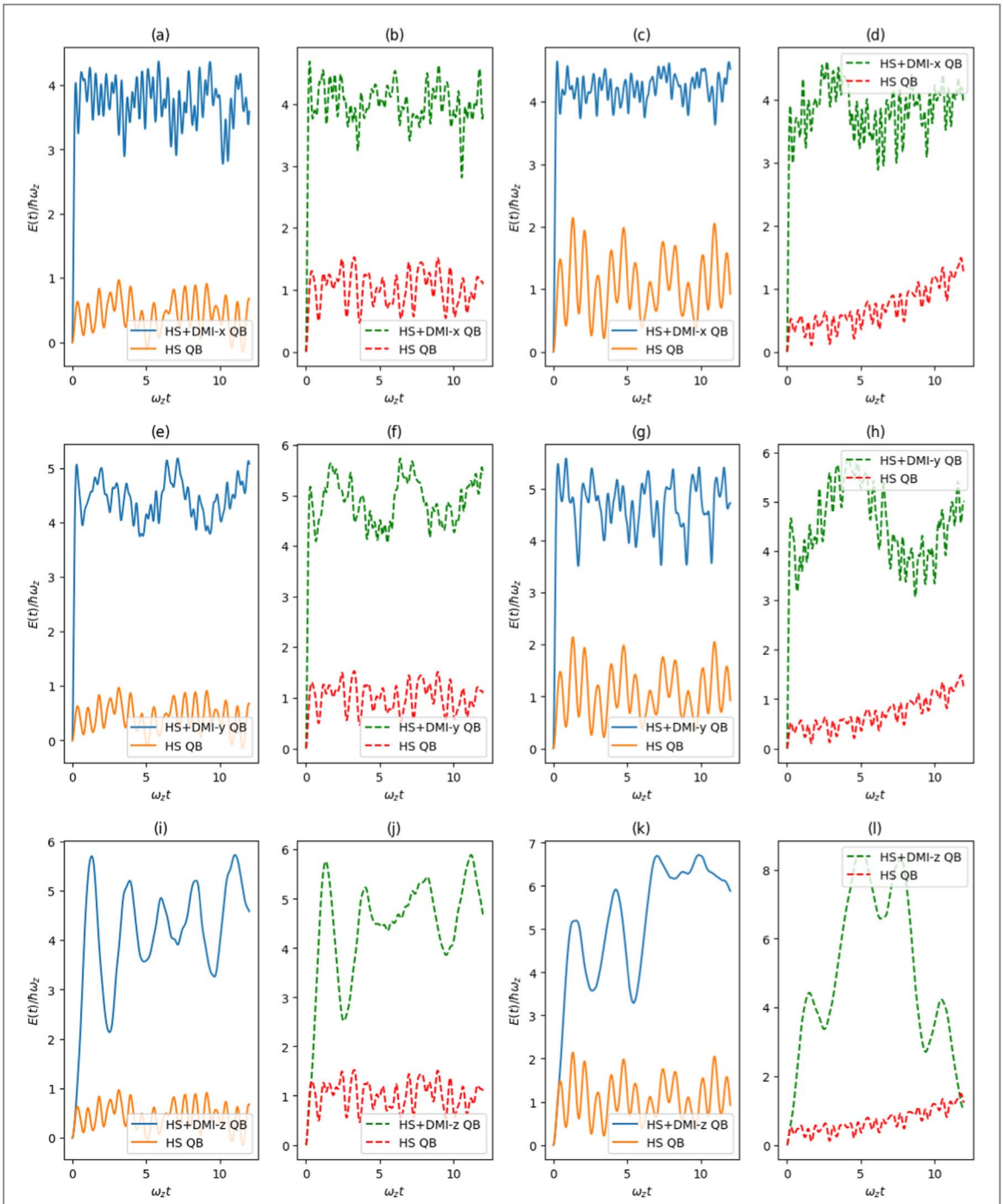

Figure 9. Total stored energy as a function of time for X, Y and Z components of DMI under infinite range interactions. (a), (b), (e), (f), (i) and (j) for local charging case and (c), (d), (g), (h), (k) and (l) for collective charging case. Here $D_z = 0.5$.

The total stored energy and the corresponding average power are plotted with the time evolution as shown in figures 9 and 10. From the figures, it is clear that there is a drastic enhancement in the total stored energy and the associated average power in the case of HS+DMI-x QB and HS+DMI-y QB as compared to HS QB. Similar trend is also observed in the case of HS+DMI-z QB for the total stored energy, except that there is only a small increment in power as compared to HS QB. Also, for the ferromagnetic case with collective charging, energy associated with HS+DMI-z QB enhances rapidly to a large value, but as time evolves the total stored energy drops down and coincides with that of HS QB.

Then the maximum stored energy and the maximum charging power are plotted as a function of N as shown in the figures 11 and 12. Here, compared to HS QB, $E_{\max}$ and $P_{\max}$ is considerably enhanced as N increases. The maximum stored energy increases linearly with the number of spins. Also, the maximum charging power appears to have a near quadratic behaviour with the number of spins in almost all cases except in the case of local charging of HS+DMI-z QB. Similar to previous studies on QBs [20, 57, 69], we expect that maximum charging power obeys the following general scaling law:

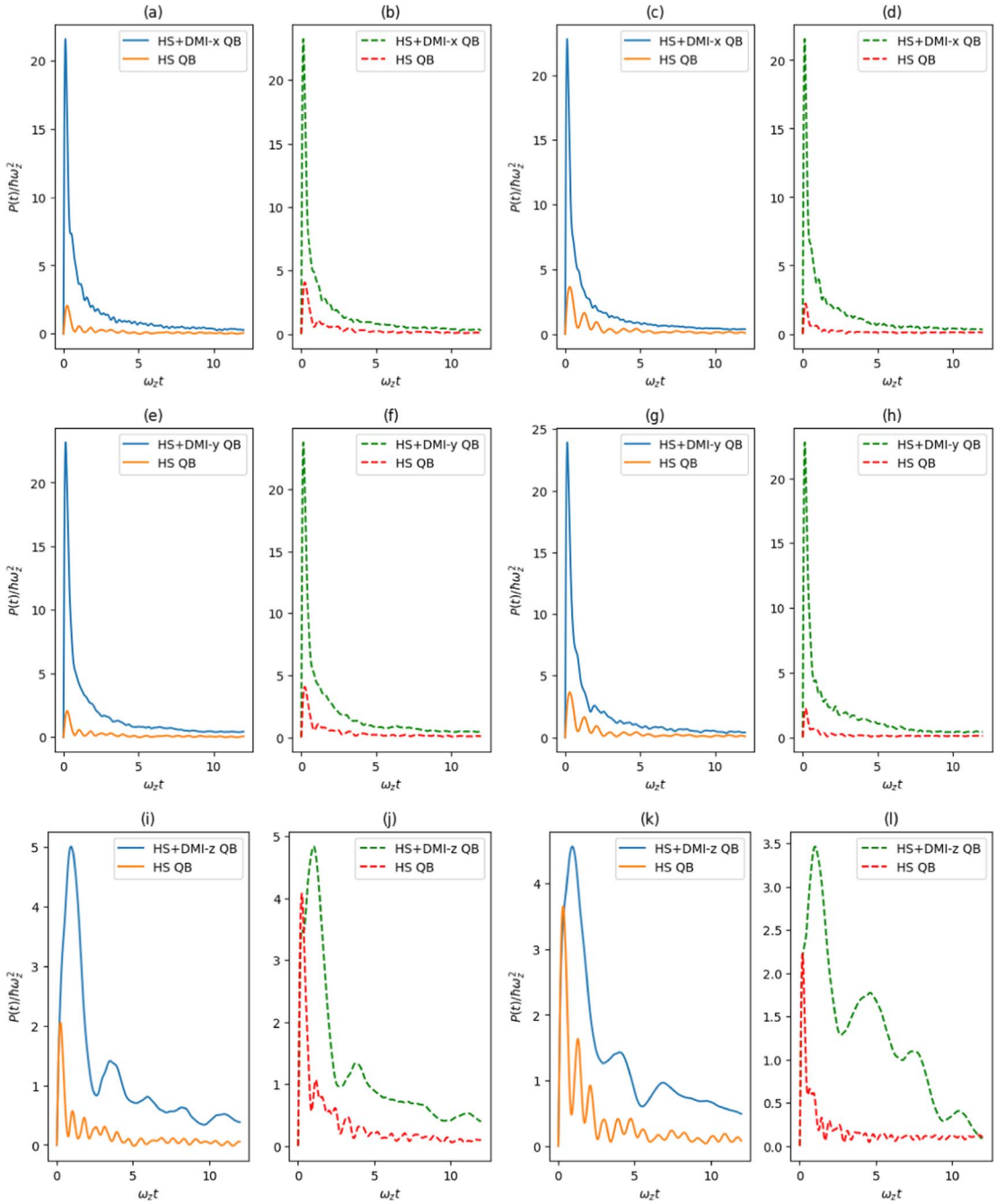

Figure 10. Average power as a function of time for X, Y and Z components of DMI under infinite range interactions. (a), (b), (e), (f), (i) and (j) for local charging case and (c), (d), (g), (h), (k) and (l) for collective charging case. Here $D_z = 0.5$.

$$P_{\max} \propto N^{\alpha} \tag{35}$$

Using linear regression, we obtain the scaling exponent α by taking logarithm as shown below.

$$\log_{10}(P_{\max}) = \alpha \log_{10}(N) + \log_{10}(C) \tag{36}$$

where C is the proportionality constant and α is referred to as the *quantum advantage* corresponding to the collective charging protocol. Similarly we can find β which is the quantum advantage corresponding to the local charging protocol.

Table 1 summarises the results obtained. We note that these magnitudes obtained are consistent with the results demonstrated in [11], further affirming that quantum charging advantage approaches quadratic scaling in the presence of interactions between the component cells in the QB.

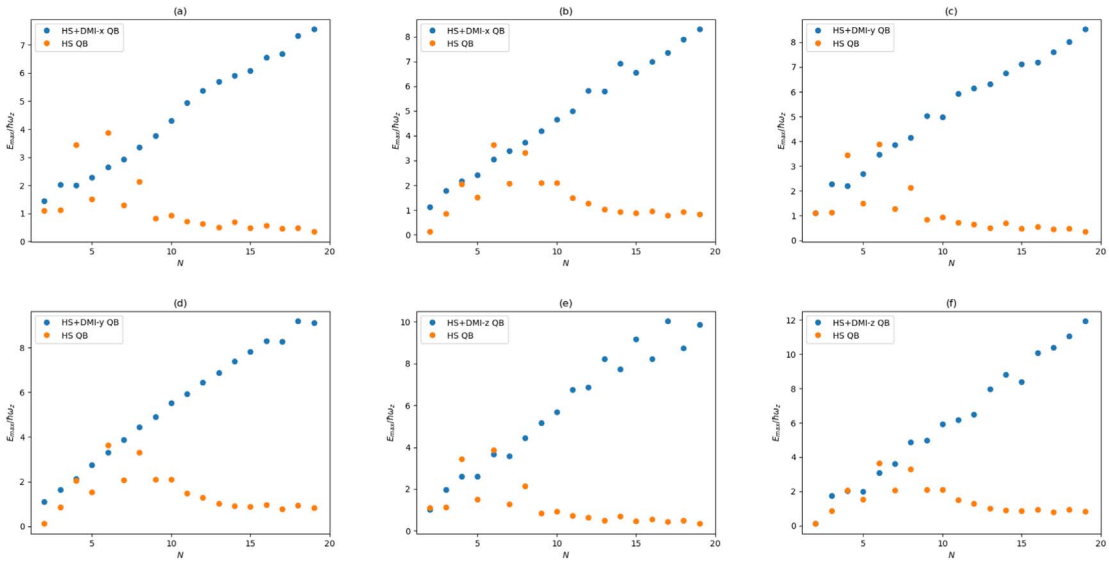

Figure 11. Maximum stored energy vs N for X, Y and Z components of DMI under infinite range interactions. (a), (c) and (e) for local charging case and (b), (d) and (f) for collective charging case.

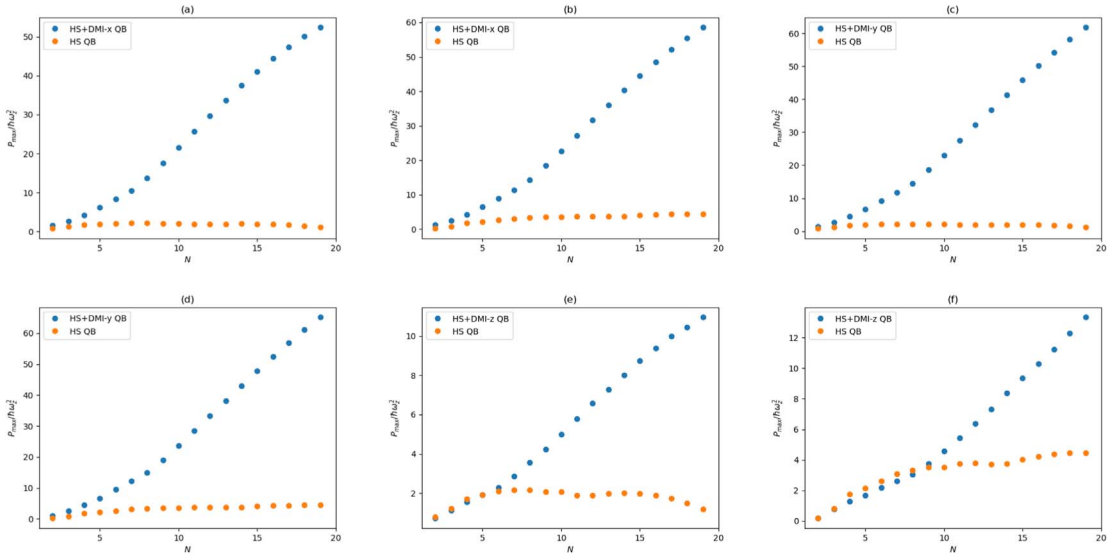

Figure 12. Maximum power vs N for X, Y and Z components of DMI under infinite range interactions. (a), (c) and (e) for local charging case and (b), (d) and (f) for collective charging case.

3. Energy fluctuations

A study on the performance of a QB is incomplete without quantifying energy quantum fluctuations, which is another figure of merit for the battery efficiency [22, 70–73]. Energy quantum fluctuations determine the quality of performance of a QB which has a direct consequence on the charging precision and ergotropy that can be achieved from a battery. According to a previous study, if each two-level system of a QB is prepared in its ground state, then an ideal charging protocol, characterized by fast charging time and the absence of charging fluctuations, can be achieved which makes the state more efficient compared to other pure preparation states [74]. Inorder to measure the energy quantum fluctuation during the charging process, we calculate the energy quantum fluctuation of the system hamiltonian ($H^{(0)}$) corresponding to a given charging protocol (ie, either local or collective charging) between the initial and final states of the battery given by the correlator,

$$V^2(t) = [\sqrt{\langle [H^{(0)}]^2(t)\rangle - [\langle H^{(0)}(t)\rangle]^2} - \sqrt{\langle [H^{(0)}]^2(0)\rangle - [\langle H^{(0)}(0)\rangle]^2}\,]^2 \tag{37}$$

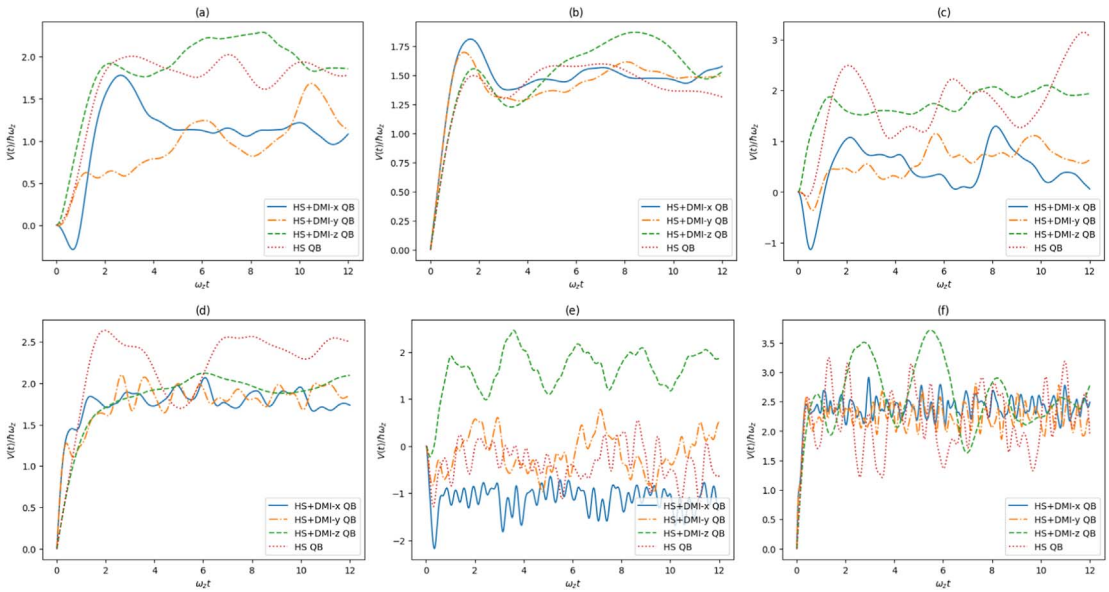

Figure 13. Energy quantum fluctuation as a function of time for X, Y and Z components of DMI for different interaction ranges. (a), (c) and (e) for local charging case and (b), (d) and (f) for collective charging case. (a) and (b) for SR, (c) and (d) for LR and (e) and (f) for IR interactions.

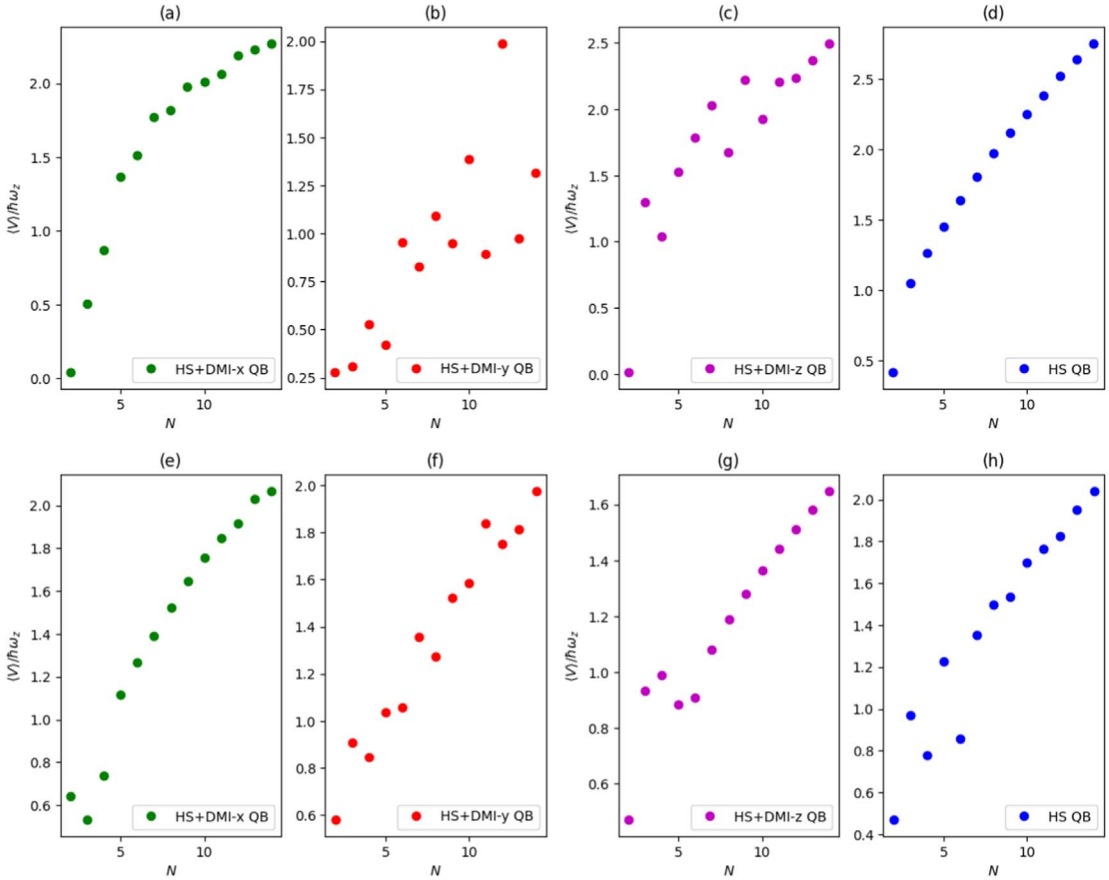

Figure 14. Energy fluctuation at time when energy is maximum vs N for X, Y and Z components of DMI under SR interactions. (a), (b), (c) and (d) for local charging case and (e), (f), (g) and (h) for collective charging case.

Then we find the value of energy quantum fluctuation at the time t_E where energy is maximum given by

$$\langle V \rangle \equiv V(t_E) \tag{38}$$

A plot of the time evolution of energy fluctuation is shown in figure 13. From the figure it is evident that there is finite amount of fluctuations present in the system for all the cases considered, and cannot be ignored. Due to

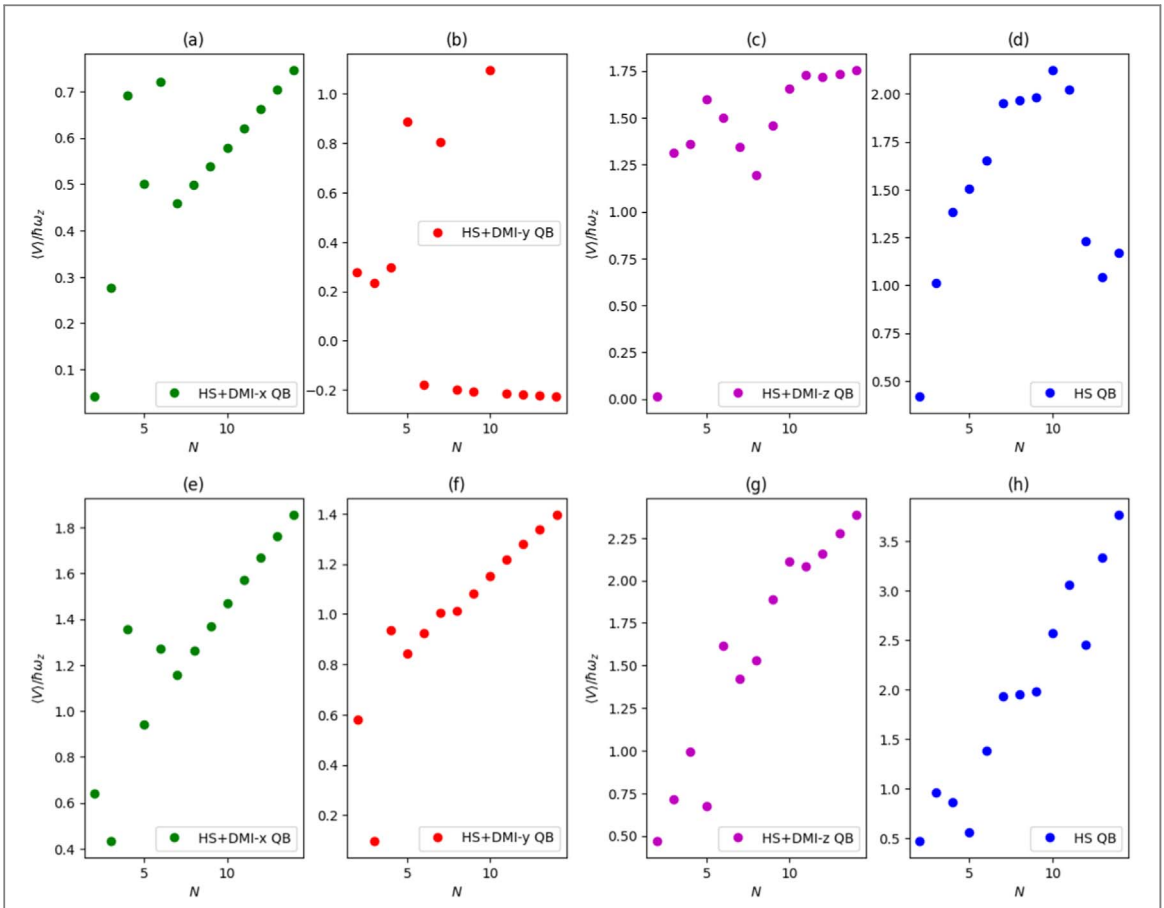

Figure 15. Energy fluctuation at time when energy is maximum vs N for X, Y and Z components of DMI under LR interactions. (a), (b), (c) and (d) for local charging case and (e), (f), (g) and (h) for collective charging case.

Table 1. Comparison of exponents α and β obtained for different QB models.

Quantum Advantage	HS QB	HS+DM-x QB	HS+DM-y QB	HS+DM-z QB
α	1.09	1.77	1.846	1.832
β	0.181	1.636	1.749	1.264

the presence of fluctuations, the QB will not be charged completely which sets limits on the availability of useful energy that can be stored/extracted from the battery (ie, ergotropy). In the case of SR interactions, local charging fluctuations are minimum for HS+DMI-x QB and HS+DMI-y QB with the evolution of time as compared to other models. But for collective charging the general trend of fluctuation is almost similar for all cases. However when we consider LR interactions, fluctuations are comparatively higher for HS QB for both charging cases out of which HS+DMI-y and HS+DMI-x models have minimal fluctuations. In the case of IR interactions, for local charging, fluctuations are higher for HS+DMI-z QB compared to other models with minimum fluctuations for HS+DMI-y QB and HS QB respectively. Similarly for the collective charging case, both HS+DMI-x QB and HS +DMI-y QB behaves in a similar manner compared to other models with larger variation in energy fluctuation for HS+DMI-z QB. Variation of $\langle V \rangle$ as a function of the number of spins, N, for different interaction ranges and charging cases are shown in figures 14, 15 and 16 respectively. From figure 14, $\langle V \rangle$ *vs* N for short range interactions, we observe that fluctuation, $\langle V \rangle$ has a clear correlation with N for both charging cases which is consistent with the results demonstrated in the previous studies [22, 70]. Hence the quantum energy fluctuation at time t_E scales linearly with the system size in the case of short range interactions. Whereas if we consider long range interactions (figure 15), in the case of collective charging, fluctuation scales with N linearly. But we cannot witness such a behaviour for local charging except that there is some regularity in the case of HS+DMI-x QB. While in the case of HS+DMI-y QB, fluctuations decreases in an irregular manner. Now if we consider the infinite range interactions as shown in figure 16, fluctuation scales with the system size for collective charging similar to the previous results but in the case of local charging, we can observe a decrease in fluctuations in the

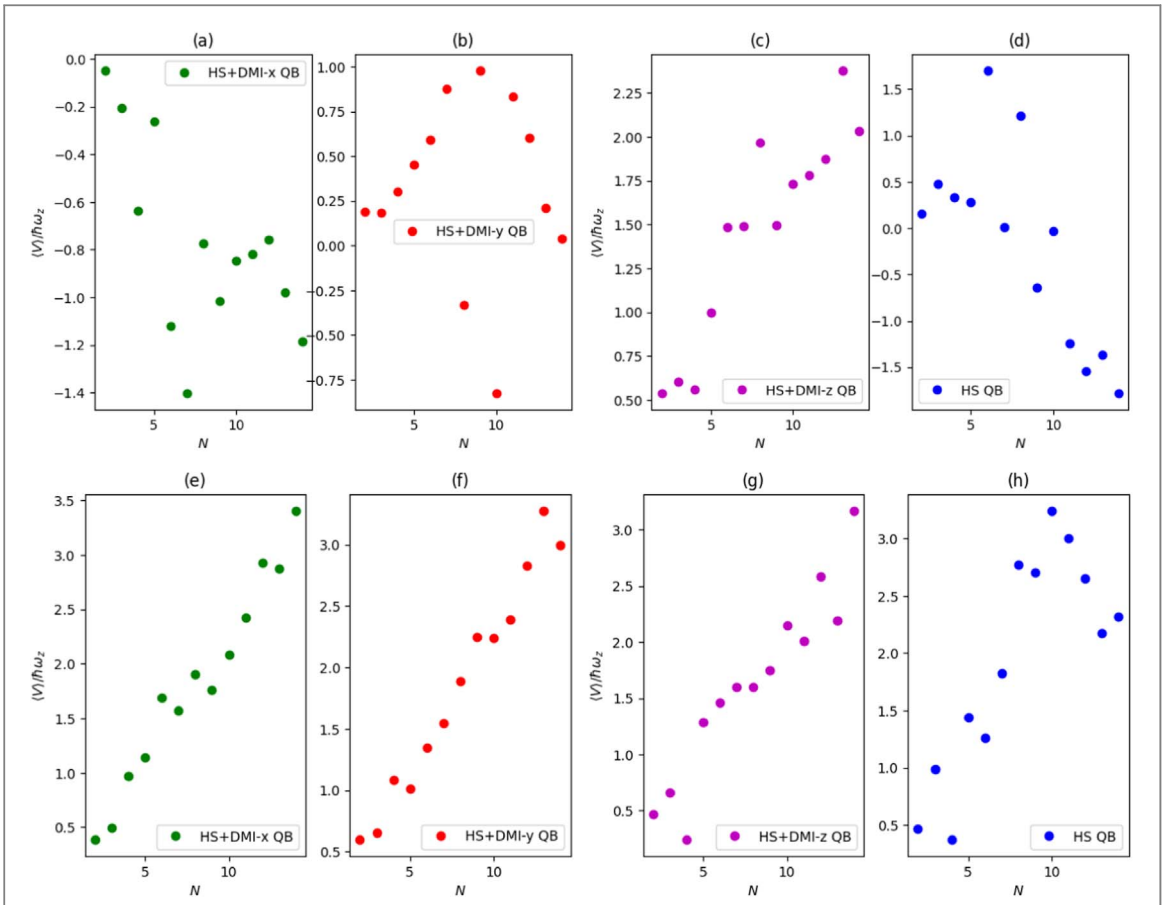

Figure 16. Energy fluctuation at time when energy is maximum vs N for X, Y and Z components of DMI under IR interactions. (a), (b), (c) and (d) for local charging case and (e), (f), (g) and (h) for collective charging case.

case of HS+DMI-x QB and HS QB. However HS+DMI-y shows an irregular behaviour, but some regularity can be seen in the case of HS+DMI-z QB in which $\langle V \rangle$ increases with N respectively.

4. Conclusions

In summary, we have considered a quantum battery model based on Heisenberg spin chain with added DM Interaction under short range, long range and infinite range interactions. In order to compare the battery performance, we have considered two types of charging protocols, namely collective and local charging. Also the effects of different components of DM Interaction (X, Y and Z component of DMI) are taken in to account. Based on this model, we have analysed the time evolution of total stored energy by the battery and the corresponding average power. Both ferromagnetic and anti-ferromagnetic cases are considered in studying the behaviour of energy and power. The maximum stored energy and maximum charging power are calculated as a function of total number of spins. Then, we measure the quantum advantage—the power exponent associated with variation in the number of cells, N—in the case of infinite range interactions. Finally, we measure the energy quantum fluctuations present in the model.

In the case of short range interactions, both X and Y components of DMI have positive effect on the battery performance while considering both energy and power compared to HS QB. Whereas there is no significant change observed in the case of HS+DMI-z QB for both charging protocols under SR interactions. In the case of long range interactions, all components of DMI enhances the total stored energy and average power except that in the case of collective charging of HS+DMI-z QB, a decline in power is observed as compared to HS QB. The total stored energy and charging power is significantly enhanced in the case of infinite range interactions as expected. In all the three cases of interaction ranges considered, HS+DMI-z QB have low average charging power than other models with DMI. Also the largest enhancement in power is achieved for IR interactions compared to SR and LR interactions.

Thereafter we find how maximum charging power and maximum stored energy scales with the number of spins. The maximum stored energy increases linearly with the number of spins in almost all cases. For SR interactions, we cannot see much difference in the behaviour of $E_{\max}$ with N. But for LR interactions, the value is

much higher compared to HS QB except in the case of collective charging of HS+DMI-z QB. In the case of IR interactions, DM interaction restores the linear scaling of $E_{\max}$ with system size unlike HS QB where $E_{\max}$ doesn't show any regularity, and compared to HS QB, the value of $E_{\max}$ tends to a high value with the increase of N. The maximum charging power also enhances with the number of spins. Compared to HS QB, $P_{\max}$ approaches a large value with N for both LR and IR interactions, except in the case of collective charging of HS+DMI-z QB for LR interactions. Also compared to other models, highest value of quantum advantage, $\alpha = 1.846$, is obtained for HS+DMI-y QB under collective charging for infinite range interactions with all to all couplings.

From the study of quantum energy fluctuations present in the system, we infer that fluctuations are inevitable in the performance of a battery out of which HS+DMI-y QB shows the least fluctuation compared to other models. Hence HS+DMI-y QB model is the most ideal model for implementation among other models of QB that we have proposed so far in terms of it's performance and figure of merits. We also studied the scaling behaviour of energy fluctuations at time when energy is maximum with the system size. In the case of collective charging, $\langle V \rangle$ scales linearly with N, but the linear behaviour is lost when the interaction range changes from SR to LR and IR interactions for the local charging case.

Acknowledgments

Sanah Rahman K acknowledges Kerala State Council for Science, Technology and Environment (KSCSTE) under the Government of Kerala for the award of KSCSTE Research fellowship (311/2022/KSCSTE).

Data availability statement

The data cannot be made publicly available upon publication because no suitable repository exists for hosting data in this field of study. The data that support the findings of this study are available upon reasonable request from the authors.

ORCID iDs

Sanah Rahman K https://orcid.org/0009-0002-5036-8092
S Murugesh https://orcid.org/0000-0002-3143-7286

References

[1] Kieu T D 2004 *Physical Review Letters* **93** 140403
[2] Uzdin R L A and Kosloff R 2016 *Entropy* **18** 124
[3] Bhattacharjee S and Dutta A 2021 *The European Physical Journal* B **94** 1–42
[4] Ferraro D, Andolina G M, Campisi M, Pellegrini V and Polini M 2019 *Physical Review* B **100** 075433
[5] Rezek Y, Salamon P, Hoffmann K H and Kosloff R 2009 *Europhysics Letters* **85** 30008
[6] Campaioli F, Pollock F A and Vinjanampathy S 2018 *Thermodynamics in the Quantum Regime: Fundamental Aspects and New Directions* 207–25
[7] Alicki R and Fannes M 2013 *Physical Review* E **87** 042123
[8] Campaioli F, Gherardini S, Quach J Q, Polini M and Andolina G M 2024 *Reviews of Modern Physics* **96** 031001
[9] Hovhannisyan K V, Perarnau-Llobet M, Huber M and Acìn A 2013 *Physical Review Letters* **111** 240401
[10] Binder F C, Vinjanampathy S, Modi K and Goold J 2015 *New Journal of Physics* **17** 075015
[11] Gyhm J Y, Šafránek D and Rosa D 2022 *Physical Review Letters* **128** 140501
[12] Santos A C 2021 *Physical Review* E **103** 042118
[13] Xu K, Zhu H J, Zhu H, Zhang G F and Liu W M 2023 *Frontiers of Physics* **18** 31301
[14] Hoang D T, Metz F, Thomasen A, Anh-Tai T D, Busch T and Fogarty T 2024 *Physical Review Research* **6** 013038
[15] Allahverdyan A E, Balian R and Nieuwenhuizen T M 2004 *Europhysics Letters* **67** 565
[16] Šafránek D, Rosa D and Binder F C 2023 *Physical Review Letters* **130** 210401
[17] Zhang Y Y, Yang T R, Fu L and Wang X 2019 *Physical Review* E **99** 052106
[18] Konar T K, Lakkaraju L G C, Ghosh S and A S 2022 *Physical Review* A **106** 022618
[19] Zhang D, Ma S, Jiang Y, Yu Y, Jin G and Chen A 2024 *Physical Review* A **110** 032211
[20] Ferraro D, Campisi M, Andolina G M, Pellegrini V and Polini M 2018 *Physical Review Letters* **120** 117702
[21] Gemme G, Andolina G M, Pellegrino F M D, Sassetti M and Ferraro D 2023 *Batteries* **9** 197
[22] Dou F Q, Lu Y Q, Wang Y J and Sun J A 2022 *Physical Review* B **105** 115405
[23] Zhang W, Wang S, Wu C and Wang G 2023 *Physical Review* E **107** 054125
[24] Downing C A and Ukhtary M S 2023 *Communications Physics* **6** 322
[25] Salvia R, Perarnau-Llobet M, Haack G, Brunner N and Nimmrichter S 2023 *Physical Review Research* **5** 013155
[26] Seah S, Perarnau-Llobet M, Haack G, Brunner N and Nimmrichter S 2021 *Physical Review Letters* **127** 100601
[27] Zhang X and Blaauboer M 2023 *Frontiers in Physics* **10** 1097564
[28] Andolina G M, Keck M, Mari A, Campisi M, Giovannetti V and Polini M 2019 *Physical Review Letters* **122** 047702

[29] Guo W X, Yang F M and Dou F Q 2024 *Physical Review* A **109** 032201
[30] Mojaveri B, Bahrbeig R J and Fasihi M A 2024 arXiv: 2405.11356
[31] Yang H Y, Shi H L, Wan Q K, Zhang K, Wang X H and Yang W L 2024 *Physical Review* A **109** 012204
[32] Ahmadi B, Mazurek P, Horodecki P and Barzanjeh S 2024 *Physical Review Letters* **132** 210402
[33] Dou F Q and Yang F M 2023 *Physical Review* A **107** 023725
[34] Qu D, Zhan X, Lin H and Xue P 2023 *Physical Review* B **108** L180301
[35] Quach J Q, McGhee K E, Ganzer L, Rouse D M, Lovett B W, Gauger E M, Keeling J, Cerullo G, Lidzey D G and Virgili T 2022 *Science Advances* **8** eabk3160
[36] Joshi J and Mahesh T 2022 *Physical Review* A **106** 042601
[37] Gautam S, Solanki S, Sharma S K, Chatzinotas S and Ottersten B 2022 *Sensors* **22** 5385
[38] Hu C K *et al* 2022 *Quantum Science and Technology* **7** 045018
[39] Gemme G, Grossi M, Ferraro D, Vallecorsa S and Sassetti M 2022 *Batteries* **8** 43
[40] Shi H L, Ding S, Wan Q K, Wang X H and Yang W L 2022 *Physical Review Letters* **129** 130602
[41] Catalano A G, Giampaolo S M, Morsch O, Giovannetti V and Franchini F 2024 *PRX Quantum* **5** 030319
[42] Rossini D, Andolina G M, Rosa D, Carrega M and Polini M 2020 *Physical Review Letters* **125** 236402
[43] Zhao F, Dou F Q and Zhao Q 2021 *Physical Review* A **103** 033715
[44] Zhao F, Dou F Q and Zhao Q 2022 *Physical Review Research* **4** 013172
[45] Quach J Q and Munro W J 2020 *Physical Review Applied* **14** 024092
[46] Mondal S and Bhattacharjee S 2022 *Physical Review* E **105** 044125
[47] Arjmandi M B, Mohammadi H and Santos A C 2022 *Physical Review* E **105** 054115
[48] Kamin F, Tabesh F, Salimi S and Santos A C 2020 *Physical Review* E **102** 052109
[49] Huangfu Y and Jing J 2021 *Physical Review* E **104** 024129
[50] Konar T K, Lakkaraju L G C and A S 2024 *Physical Review* A **109** 042207
[51] Ghosh S, Chanda T, Mal S and A S 2021 *Physical Review* A **104** 032207
[52] Grazi R, Shaikh D S, Sassetti M, Ziani N T and Ferraro D 2024 *Physical Review Letters* **133** 197001
[53] Yao Y and Shao X 2022 *Physical Review* E **106** 014138
[54] Mojaveri B, Jafarzadeh Bahrbeig R and Fasihi M 2024 *Physical Review* A **109** 042619
[55] Barra F, Hovhannisyan K V and Imparato A 2022 *New Journal of Physics* **24** 015003
[56] Rossini D, Andolina G M and Polini M 2019 *Physical Review* B **100** 115142
[57] Dou F Q, Zhou H and Sun J A 2022 *Physical Review* A **106** 032212
[58] Le T P, Levinsen J, Modi K, Parish M M and Pollock F A 2018 *Physical Review* A **97** 022106
[59] Ghosh S *et al* 2020 *Physical Review* A **101** 032115
[60] Ali A, Al-Kuwari S, Hussain M, Byrnes T, Rahim M, Quach J Q, Ghominejad M and Haddadi S 2024 *Physical Review A* **110** 052404
[61] Zhang X L, Song X K and Wang D 2024 *Advanced Quantum Technologies* 2400114
[62] Ghosh S *et al* 2022 *Physical Review* A **105** 022628
[63] Moriya T 1960 *Physical Review* **120** 91
[64] Moriya T 1960 *Physical Review Letters* **4** 228
[65] Hälg M, Lorenz W E, Povarov K Y, Månsson M, Skourski Y and Zheludev A 2014 *Physical Review* B **90** 174413
[66] Mazzoncini F, Cavina V, Andolina G M, Erdman P A and Giovannetti V 2023 *Physical Review* A **107** 032218
[67] Polkovnikov A, Sengupta K, Silva A and Vengalattore M 2011 *Reviews of Modern Physics* **83** 863
[68] Johansson J R, Nation P D and Nori F 2012 *Computer Physics Communications* **183** 1760–72
[69] Campaioli F, Pollock F A, Binder F C, Céleri L, Goold J, Vinjanampathy S and Modi K 2017 *Physical review letters* **118** 150601
[70] Crescente A, Carrega M, Sassetti M and Ferraro D 2020 *Physical Review* B **102** 245407
[71] Rosa D, Rossini D, Andolina G M, Polini M and Carrega M 2020 *Journal of High Energy Physics* **2020**
[72] Garcìa-Pintos L P, Hamma A and Del Campo A 2020 *Physical Review Letters* **125** 040601
[73] Friis N and Huber M 2018 *Quantum* **2** 61
[74] Crescente A, Carrega M, Sassetti M and Ferraro D 2020 *New Journal of Physics* **22** 063057